

# Shell model calculations for light supersymmetric particle scattering off light nuclei

P. C. Divari, T. S. Kosmas, and J. D. Vergados

*Department of Physics, University of Ioannina, GR-45110 Ioannina, Greece*

L. D. Skouras

*Institute of Nuclear Physics, NCSR Demokritos, GR-15310 Aghia Paraskevi, Greece*

(Received 7 September 1999; published 12 April 2000)

We investigate the elastic scattering cross section of cold dark matter candidates, i.e., lightest supersymmetric particles (LSP), with light nuclei ( $^{19}\text{F}$ ,  $^{23}\text{Na}$ , and  $^{29}\text{Si}$ ). These nuclei are promising targets of direct detection for such cold dark matter. We pay special attention to the spin dependence of the differential event rate. Our calculations are performed in the  $s$ - $d$  shell model space with the Wilthenthal interaction. We also examine the momentum transfer dependence of the differential cross section.

PACS number(s): 23.40.Hc, 23.40.Bw, 21.60.Cs, 21.60.Jz

## I. INTRODUCTION

It is known that dark matter is needed to close the Universe [1,2]. It is customary to define the parameter  $\Omega$  given by

$$\Omega = \frac{\rho}{\rho_c}, \quad \rho_c = \frac{3H^2}{8\pi G_N}, \quad (1)$$

where  $\rho$  is the density of the Universe,  $\rho_c$  the critical density,  $H$  the Hubble constant, and  $G_N$  the Newton's gravitational constant. Then, one theoretically expects  $\Omega \cong 1$ , while the usual (baryonic) matter gives  $\Omega_B \leq 0.1$ . In order to accommodate  $\Omega \cong 1$ , nonluminous (dark) matter is needed. Two types of such matter have been considered. The first is composed of particles which were relativistic at the time of structure formation and constitutes the hot dark matter component (HDM). The other type is made up of particles which were nonrelativistic at the time of freeze out and constitutes the cold dark matter component (CDM). The COBE data [3] suggest that CDM is at least 60% [4]. On the other hand recent data from the Supernova Cosmology Project suggest [5,6] that there is no need for HDM and the situation can be adequately described by  $\Omega_{CDM} = 0.3$  and  $\Omega_\Lambda = 0.6$  ( $\Omega_\Lambda$  is associated with the cosmological constant). In any case the presence of CDM seems unavoidable.

Since the nonexotic component cannot exceed 40% of the CDM [2,7], there is room for the exotic weakly interacting massive particles (WIMP's). The direct detection of such particles is thus of profound importance. Recently, the DAMA experiment [8] has claimed the observation of one signal in direct detection of a WIMP, which with better statistics has subsequently been interpreted as a modulation signal [9].

In the currently favored supersymmetric (SUSY) extensions of the standard model the most natural WIMP candidate is the LSP, i.e., the lightest supersymmetric particle whose nature can be described in most SUSY models to be a Majorana fermion, a linear combination of the neutral components of the gauginos and Higgsinos [10–12] with mass greater than  $30 \text{ GeV}/c^2$ . It is nonrelativistic with an average

energy less than 100 keV. In practice, however, one expects the LSP to have a velocity distribution which is supposed to be Maxwellian [2].

The detection of the LSP, which in the following is denoted by  $\chi$ , is quite difficult, since this particle interacts extremely weakly with matter. The most interesting possibility for a direct detection of the LSP is via the recoiling of the nucleus ( $A, Z$ ) in the process

$$\chi + (A, Z) \rightarrow \chi + (A, Z)^*.$$

In the above process only the elastic channel is of practical interest, since either the energy of LSP is too low to excite the nucleus or the cross section is too low to be measured. Among the most popular detector nuclei ( $^A_Z X$ ) are the following isotopes:  $^3_2\text{He}$ ,  $^{19}_9\text{F}$ ,  $^{23}_{11}\text{Na}$ ,  $^{27}_{13}\text{Al}$ ,  $^{29}_{14}\text{Si}$ ,  $^{40}_{20}\text{Ca}$ ,  $^{73}_{32}\text{Ge}$ ,  $^{75}_{33}\text{As}$ ,  $^{127}_{53}\text{I}$ ,  $^{134}_{54}\text{Xe}$ , and  $^{208}_{82}\text{Pb}$ .

The theoretical expression for the LSP-nucleus cross section includes basically two parts: the coherent part, coming mainly from the scalar interaction, and the spin contribution coming from the axial current. The coherent contribution is expected to dominate in the case of heavy targets, but the spin matrix element (ME) may be more important in the case of light nuclear systems.

The coherent matrix elements can easily be described in terms of the nuclear form factor and computed approximately throughout the periodic table [13], but the evaluation of the spin matrix elements is more complicated. The cross sections at zero momentum transfer ( $q \equiv |\mathbf{q}| = 0$ ) show a strong dependence on the nuclear structure of the ground state.

It is the purpose of this paper to present results of calculations for the static spin matrix elements and at the same time to explore their momentum transfer dependence.

Initial investigations into the spin-dependent  $\chi$ -nucleus scattering made use of the independent single particle shell model (ISPSM) [14–17]. Engel and Vogel [18], employing the extended odd group model (EOGM), evaluated the spin ME using data from magnetic moments and mirror pair  $\beta$  decays. They showed that the ISPSM was inadequate, when nuclei are far from the closed shells (see also Ref. [19]). Pacheco and Strottman [20] reached the same conclu-

sion by performing detailed nuclear shell model calculations for several light nuclei. The odd group model (OGM) and shell model treatments obtain good agreement for light nuclei but as the atomic mass increases, there is a significant amount of configuration mixing which is not considered in the OGM. The authors of Ref. [21] employed the interaction boson fermion model (IBFM), in order to evaluate the spin matrix elements. While the IBFM can incorporate the dominant collective effects, it has some difficulty in including the spin polarization which plays a crucial role in axial vector scattering. In addition it cannot be readily applied at nonzero momentum transfer.

It is evident from the above discussion that there is need for more detailed calculations going beyond the IPSM, especially for the spin component of the cross section. The main aim of the present paper is to evaluate the spin response upon the cross section in  $\chi$ -nucleus scattering making a shell model calculation restricted to the light nuclei  $^{19}\text{F}$ ,  $^{23}\text{Na}$ , and  $^{29}\text{Si}$ , which are among the popular nuclei as detector candidates. A similar calculation for  $^{29}\text{Si}$  and  $^{73}\text{Ge}$  was performed by Ressel *et al.* [22]. The advantages of our approach will be exhibited in Secs. II B and IV B.

While phenomenological models, like the OGM and IBFM which have been used in the  $q=0$  limit, cannot be easily extended to finite momentum transfer, in a nuclear shell model calculation the incorporation of finite momentum transfer is straightforward. In fact it can be described as a low degree polynomial in  $q^2$  times a Gaussian (see Sec. II).

## II. THE BASIC INGREDIENTS FOR LSP NUCLEUS SCATTERING

In this section we shall state in brief the main steps followed for the construction of the  $\chi$ -nucleus interaction Hamiltonian in the context of supersymmetry. Then, we will describe the formalism employed for the evaluation of the spin matrix element and the spin form factors which are of primary importance in our study.

### A. Effective operators at the nucleon level

The  $\chi$ -nucleus scattering can be described by a four-fermion interaction of the type [10]

$$L_{\text{eff}} = -\frac{G_F}{\sqrt{2}} \{ (\bar{\chi}\gamma^\lambda\gamma_5\chi)J_\lambda + (\bar{\chi}\chi)J \}, \quad (2)$$

where

$$J_\lambda = \bar{N}\gamma_\lambda(f_V^0 + f_V^1\tau_3 + f_A^0\gamma_5 + f_A^1\gamma_5\tau_3)N \quad (3)$$

and

$$J = \bar{N}(f_S^0 + f_S^1\tau_3)N \quad (4)$$

( $N$ =nucleon spinor). The effective Lagrangian can be obtained in first order via Higgs exchange,  $s$ -quark exchange, and  $Z$  exchange. In the above expressions we have neglected the uninteresting pseudoscalar and tensor currents. We mention that, due to the Majorana nature of the LSP, we have

$\bar{\chi}\gamma^\lambda\chi = 0$ . The parameters  $f_V^0, f_V^1, f_A^0, f_A^1, f_S^0, f_S^1$ , depend on the specific SUSY model employed [10].

The corresponding  $\chi$ -nucleus differential cross section in the laboratory frame takes the form [10]

$$\frac{d\sigma}{d\Omega} = \frac{\sigma_0}{\pi} \left( \frac{\mu_r}{m_N} \right)^2 \xi (|\mathbf{J}|^2 + |J|^2), \quad (5)$$

with the spin contribution given by

$$|\mathbf{J}|^2 = \frac{1}{2J_i + 1} |\langle J_i | [f_A^0 \mathbf{\Omega}_0(\mathbf{q}) + f_A^1 \mathbf{\Omega}_1(\mathbf{q})] | J_i \rangle|^2 \quad (6)$$

and the coherent (scalar) one (neglecting the small component associated with the time component of the vector current) is given by

$$|J|^2 = A^2 \left( f_S^0 - f_S^1 \frac{A-2Z}{A} \right)^2 |F(\mathbf{q}^2)|^2. \quad (7)$$

$F(\mathbf{q}^2)$  is the nuclear form factor and

$$\mathbf{\Omega}_0(\mathbf{q}) = \sum_{j=1}^A \boldsymbol{\sigma}(j) e^{-i\mathbf{q}\cdot\mathbf{x}_j}, \quad \mathbf{\Omega}_1(\mathbf{q}) = \sum_{j=1}^A \boldsymbol{\sigma}(j) \tau_3(j) e^{-i\mathbf{q}\cdot\mathbf{x}_j}, \quad (8)$$

$\boldsymbol{\sigma}(j)$ ,  $\tau_3(j)$ ,  $\mathbf{x}_j$  are the spin, third component of isospin ( $\tau_3|p\rangle = |p\rangle$ ), and the coordinate of the  $j$ th nucleon.

In Eq. (5)  $\sigma_0$  is given by

$$\sigma_0 = \frac{1}{2\pi} (G_F m_N)^2 \approx 0.77 \times 10^{-38} \text{ cm}^2, \quad (9)$$

while  $\mu_r$  is the reduced mass of the LSP-nucleus system and  $m_N$  is the proton mass. Furthermore,  $\xi = \hat{\mathbf{p}}_i \cdot \hat{\mathbf{q}} \geq 0$  (forward scattering) with the momentum transfer  $\mathbf{q}$  given by

$$|\mathbf{q}| = q_0 \xi, \quad q_0 = 2\beta c \mu_r, \quad \beta = v/c. \quad (10)$$

For the evaluation of the differential rate it is more convenient to use the variables  $(u, v)$  instead of the variables  $(\xi, v)$  where  $u$  is defined by

$$u = (qb)^2/2 \quad (11)$$

with  $b$  being the oscillator size parameter. The above defined quantity  $u$  is related to the energy transfer to the nucleus  $Q$  as follows:

$$Q = Q_0 u, \quad Q_0 = \frac{1}{Am_N b^2}. \quad (12)$$

Thus, integrating the differential cross section of Eq. (5), with respect to the azimuthal angle we obtain

$$d\sigma(u, v) = \sigma_0 \left( \frac{\mu_r}{m_N} \right)^2 \left[ (f_A^1)^2 F_{11}(u) S(u) + A^2 \left( f_S^0 - f_S^1 \frac{A-2Z}{A} \right)^2 |F(u)|^2 \right] \frac{du}{2(\mu_r b v)^2}, \quad (13)$$

where

$$S(u) = \left( \frac{f_A^0}{f_A^1} \right)^2 \frac{F_{00}(u)}{F_{11}(u)} (\Omega_0(0))^2 + 2 \frac{f_A^0}{f_A^1} \frac{F_{01}(u)}{F_{11}(u)} \Omega_0(0) \Omega_1(0) + (\Omega_1(0))^2 \quad (14)$$

and

$$F_{\rho\rho'}(u) = \sum_{\lambda, k} \frac{\Omega_\rho^{(\lambda, \kappa)}(u)}{\Omega_\rho(0)} \frac{\Omega_{\rho'}^{(\lambda, \kappa)}(u)}{\Omega_{\rho'}(0)}, \quad \rho, \rho' = 0, 1 \quad (15)$$

are the spin form factors, associated with isospin indices  $\rho, \rho'$ , which take values 0 and 1. The quantities  $\Omega_\rho^{(\lambda, k)}(u)$  will be discussed below [ $\Omega_\rho(0) \equiv \Omega_\rho^{(0,1)}(0)$  is the static value of the spin ME].

In Eq. (14) we have introduced the quantity  $S(u)$ , which contains most of the nuclear structure information, because we expect it to be essentially independent of  $u$  (see below Sec. II B), i.e., nearly static quantity  $S(u) \approx S(0)$ . It will also depend less strongly on the SUSY parameters, since it is expressed in terms of the ratio  $f_A^0/f_A^1$  and therefore the dependence of each one of them on the not so well known SUSY mass scale will tend to cancel in the ratio.

The parameter  $f_A^1$  in Eq. (13), which, among other things, depends on the inverse of the second power of the mass of the intermediate particles, is not going to be discussed further in this work (see, e.g., Ref. [10]). The momentum transfer dependent quantity  $F_{11}(u)$  is extensively discussed below.

We will demonstrate in the present paper that it is advantageous to separate the static values from the ‘‘spin form factors.’’ Before concluding this section, however, for the reader’s convenience we mention that sometimes, see, e.g., Ressel *et al.* [22], the first term of Eq. (13) of the spin contribution can be written in the form

$$d\sigma = \frac{8G_F^2}{(2J_i+1)v^2} h(q) dq^2, \quad (16)$$

where  $h(q)$  is the spin structure function, which may be split into a pure isoscalar piece  $S_{00}$ , a pure isovector piece  $S_{11}$ , and an interference term  $S_{01}$ , in the following way:

$$h(q) = \frac{1}{4} [(f_A^0)^2 S_{00}(q) + (f_A^1)^2 S_{11}(q) + f_A^0 f_A^1 S_{01}(q)]. \quad (17)$$

If we combine the first term of Eq. (13) with Eq. (16) we can take the following relations between  $S_{\rho\rho'}(q)$  and  $F_{\rho\rho'}(u)$ :

$$S_{\rho\rho}(q) = (2J_i+1) \frac{1}{16\pi} [\Omega_\rho(0)]^2 F_{\rho\rho}(u), \quad \rho=0,1 \quad (18)$$

and

$$S_{01}(q) = (2J_i+1) \frac{1}{8\pi} [\Omega_0(0)\Omega_1(0)] F_{01}(u). \quad (19)$$

## B. Expressions for the spin matrix element

The determination of the spin matrix element  $|\mathbf{J}|^2$  of Eq. (6), relies on the calculation of the multiparticle reduced matrix elements of the operator

$$\mathbf{O}^{(\lambda,1)k} \equiv \mathbf{O}^{(\lambda,k)} = (f_A^0 + f_A^1 \tau_3) \mathbf{T}^{(\lambda,k)}, \quad (20)$$

where

$$\mathbf{T}^{(\lambda,k)} = \sqrt{4\pi} j_\lambda(qr) [Y_\lambda(\hat{r}) \times \boldsymbol{\sigma}]^k \quad (21)$$

(Gamow-Teller-type operators) sandwiched between the many-body wave functions for the initial ( $|J_i\rangle$ ) and final ( $|J_f\rangle$ ) nuclear states. In the multiparticle basis the reduced matrix elements of the operator  $\mathbf{O}^{(\lambda,k)}$  contain isoscalar and isovector components as

$$\frac{\langle J_f || \mathbf{O}^{(\lambda,k)} || J_i \rangle}{[2J_i+1]^{1/2}} = f_A^0 \Omega_0^{(\lambda,k)}(q) + f_A^1 \Omega_1^{(\lambda,k)}(q), \quad (22)$$

where  $\Omega_\rho^{(\lambda,k)}(q)$  represent the isoscalar ( $\rho=0$ ) and isovector ( $\rho=1$ ) contributions, respectively, expressed as

$$\Omega_\rho^{(\lambda,k)}(q) = \sum_{j_1 j_2} \alpha_\rho^k(j_1 j_2) \frac{\langle j_1 || \mathbf{T}^{(\lambda,k)} || j_2 \rangle}{[2J_i+1]^{1/2}}, \quad \rho=0,1. \quad (23)$$

Note the presence of  $(2J_i+1)^{-1/2}$  in the definition of the above matrix elements in terms of the reduced matrix elements. In other words the matrix elements are written in terms of the quantities  $\alpha_\rho^k(j_1 j_2)$ , which carry all the information about the interaction and the single-particle reduced matrix elements of  $\mathbf{T}^{(\lambda,k)}$ . The indices  $j_1$  and  $j_2$  run over the single-particle orbits of the chosen model space. The quantities  $\alpha_\rho^k(j_1 j_2)$ , which are essentially products of the one body coefficients of fractional parentage (CFP), are sometimes called one-body transition amplitudes [26]. For elastic scattering we need consider only the case  $|J_f\rangle = |J_i\rangle \equiv |gs\rangle$ , where  $|gs\rangle$  is the nuclear ground state which for  $^{19}\text{F}$  and  $^{29}\text{Si}$  is a  $J^\pi = 1/2^+$  while for  $^{23}\text{Na}$  is a  $J^\pi = 3/2^+$  state. The values of  $\alpha_\rho^k(j_1 j_2)$ , which depend, of course, on the specific interaction and the model space used, are given in Table I for each of the studied nucleus and for the necessary values of  $k$ .

The momentum dependence of the matrix elements Eq. (23) can be simply obtained by using the convenient expressions for the single-particle reduced matrix elements of the operator  $\mathbf{T}^{(\lambda,k)}$  evaluated in the harmonic oscillator basis (see

TABLE I. The one-body transition amplitudes  $\alpha_\rho^k(j_1j_2)$  of Eq. (23) for ordered pairs  $(j_1j_2)$  calculated in the  $s$ - $d$  shell model space with the Wildenthal interaction of Ref. [23]. Note that  $\alpha_\rho^k(j_1j_2) = (-)^{j_1+j_2+1}\alpha_\rho^k(j_2j_1)$ .

$^{19}\text{F}$		$^{29}\text{Si}$			
$j_1j_2$	$\alpha_0^{k=1}(j_1j_2)$	$\alpha_1^{k=1}(j_1j_2)$	$\alpha_0^{k=1}(j_1j_2)$	$\alpha_1^{k=1}(j_1j_2)$	
$d_{5/2}-d_{5/2}$	0.122791	0.240873	0.115158	-0.111104	
$d_{3/2}-d_{3/2}$	-0.054308	-0.012108	-0.080300	0.087330	
$s_{1/2}-s_{1/2}$	0.445327	0.408141	0.572650	-0.552962	
$d_{5/2}-d_{3/2}$	-0.121695	-0.105475	0.196288	-0.185400	
$d_{5/2}-s_{1/2}$					
$d_{3/2}-s_{1/2}$	-0.011985	0.012797	0.024895	-0.014197	
$^{23}\text{Na}$					
$\alpha_0^{k=1}(j_1j_2)$	$\alpha_1^{k=1}(j_1j_2)$	$\alpha_0^{k=2}(j_1j_2)$	$\alpha_1^{k=2}(j_1j_2)$	$\alpha_0^{k=3}(j_1j_2)$	$\alpha_1^{k=3}(j_1j_2)$
0.498455	0.291611	-0.549368	0.116516	-0.526623	-0.538119
0.101504	0.030846	-0.031558	-0.014947	0.059510	0.085382
-0.107601	-0.096975				
-0.057835	-0.099517	-0.289246	0.073162	0.055927	0.081597
		-0.586684	-0.098876	0.042913	0.057059
-0.017184	-0.072502	0.163744	-0.046236		

Appendix). Thus, replacing the corresponding expressions of  $\langle j_1 || \mathbf{T}^{(\lambda,k)} || j_2 \rangle$  for the  $s$ - $d$  shell in Eq. (23) we find

$$\Omega_\rho^{(0,1)}(u) = \Omega_\rho(0) P_\rho^{(0,1)}(u) e^{-u/2}, \quad (24)$$

$$\Omega_\rho^{(2,k)}(u) = \Omega_\rho(0) P_\rho^{(2,k)}(u) e^{-u/2}, \quad k=1,2,3, \quad (25)$$

$$\Omega_\rho^{(4,3)}(u) = \Omega_\rho(0) P_\rho^{(4,3)}(u) e^{-u/2}, \quad (26)$$

where  $P_\rho^{(\lambda,\kappa)}(u)$  polynomials in  $u$  given by

$$P_\rho^{(0,1)}(u) = \left( \frac{1}{15} + \lambda_\rho \right) u^2 - \frac{2}{3} u + 1, \quad (27)$$

$$P_\rho^{(2,1)}(u) = D_\rho u^2 + C_\rho u, \quad P_\rho^{(2,2)}(u) = 0.0, \quad (28)$$

$$P_\rho^{(2,3)}(u) = F_\rho u^2 + E_\rho u,$$

$$P_\rho^{(4,3)}(u) = A_\rho u^2. \quad (29)$$

The values of the coefficients  $\lambda_\rho$ ,  $D_\rho$ ,  $C_\rho$ ,  $E_\rho$ ,  $F_\rho$ , and  $A_\rho$  are given in Table II. Using Eqs. (24)–(29) the spin matrix element  $|\mathbf{J}|^2$  of Eq. (6) takes the form

$$|\mathbf{J}|^2 = \sum_{\rho,\rho'} f_A^\rho f_A^{\rho'} \Omega_\rho(0) \Omega_{\rho'}(0) F_{\rho\rho'}(u). \quad (30)$$

We see that, the momentum dependence of the spin form factor is contained in the structure functions  $F_{\rho\rho'}(u)$ . For the nuclear systems we examine in the present paper these functions take the general form

$$F_{\rho\rho'}(u) = [P_\rho^{(0,1)}(u) P_{\rho'}^{(0,1)}(u) + P_\rho^{(2,1)}(u) P_{\rho'}^{(2,1)}(u) + P_\rho^{(2,3)}(u) P_{\rho'}^{(2,3)}(u) + P_\rho^{(4,3)}(u) P_{\rho'}^{(4,3)}(u)] e^{-u}. \quad (31)$$

Since  $F_{\rho\rho'}(u)$  are normalized to unity at zero momentum transfer ( $u=0$ ), they have a behavior similar in all isospin channels, that is  $F_{\rho\rho'}(u)/F_{11}(u) \approx 1$ , for  $\rho, \rho' = 0, 1$ . It is thus

TABLE II. The basic ingredients required for the evaluation of the spin matrix elements [see Eqs. (27)–(29)], as well as the parameters  $\zeta$ ,  $\beta_{csm}$ , and  $\delta$  entering the nuclear form factor, Eq. (42).

	$^{19}\text{F}$	$^{29}\text{Si}$	$^{23}\text{Na}$
$\lambda_0$	0.0477	0.2176	-0.0190
$\lambda_1$	0.0421	0.2043	-0.0202
$D_0$	-0.0026	-0.0567	-0.0177
$D_1$	0.0006	-0.0621	-0.0349
$C_0$	0.0100	0.4566	0.1048
$C_1$	0.0041	0.4680	0.1494
$F_0$			-0.0767
$F_1$			-0.0894
$E_0$			0.6092
$E_1$			0.7405
$A_0$			0.0221
$A_1$			0.0287
$\zeta$	$\frac{6}{19}$	$\frac{38}{87}$	$\frac{26}{69}$
$\beta_{csm}$	0	$\frac{26}{435}$	0
$\delta$	0.0170	-0.0241	0.0250

convenient to express our results of the differential rate in terms of the quantities  $f_A^1$ ,  $F_{11}(u)$ , and  $S(u)$ . Notice that, since the ratios  $F_{\rho\rho'}(u)/F_{11}(u)$  are almost unity the quantity  $S(u)$  is essentially static, i.e.,  $S(u) \approx S(0)$ . For this reason it has been defined as in Eq. (14). It is, thus, advantageous to use our functions  $F_{\rho\rho'}(u)$  as opposed to the functions  $S_{\rho\rho'}(y)$  used in Ref. [22] [see Eqs. (18) and (19)], in which this separation is not made.

Before closing this section we should mention a very subtle point. It is fairly well known that at relatively high momentum transfer the nucleonic axial current, due to partially conserved axial current (PCAC) considerations, gets modified in the following way:

$$\boldsymbol{\sigma} \rightarrow \left[ \boldsymbol{\sigma} - \frac{(\boldsymbol{\sigma} \cdot \mathbf{q})\mathbf{q}}{q^2 + m_\pi^2} \right],$$

where  $m_\pi$  is the pion mass. Thus, the above results are modified in two ways: (i) There is now interference between the various operators of the same  $k$  but different orbital ranks  $\lambda$ . (ii) The diagonal matrix elements get quenched for relatively high momentum transfer. These modifications will be discussed in detail elsewhere, when we are going to study the differential event rate as a function of  $u$ . For the reader's convenience, however, we give here a summary of the results only for the  $J^\pi = 1/2^+$  nuclei, that is for the isotopes  $^{19}\text{F}$  and  $^{29}\text{Si}$ . In this case it is easy to show that the structure functions  $F_{\rho\rho'}(u)$  are given by the expression

$$\begin{aligned} F_{\rho\rho'}(u) = & \{ P_\rho^{(0,1)}(u) P_{\rho'}^{(0,1)}(u) [1 + \beta_0(u)] \\ & + P_\rho^{(2,1)}(u) P_{\rho'}^{(2,1)}(u) [1 + \beta_2(u)] - \beta_{02}(u) \\ & \times [P_\rho^{(0,1)}(u) P_{\rho'}^{(2,1)}(u) + P_\rho^{(2,1)}(u) P_{\rho'}^{(0,1)}(u)] \} e^{-u}, \end{aligned} \quad (32)$$

with

$$\begin{aligned} \beta_0(u) = & \frac{1}{3} \left[ \left( \frac{u_\pi}{u + u_\pi} \right)^2 - 1 \right], \quad \beta_2(u) = \frac{2}{3} \left[ \left( \frac{u_\pi}{u + u_\pi} \right)^2 - 1 \right], \\ \beta_{02}(u) = & \frac{\sqrt{2}}{3} \frac{u(u + 2u_\pi)}{(u + u_\pi)^2}, \end{aligned} \quad (33)$$

where  $u_\pi = (1/2)(bm_\pi)^2$ . Note that, in the limit when the pion mass can be considered infinite, we find that the  $\beta_0$ ,  $\beta_2$ , and  $\beta_{02}$  go to zero and we recover the results of Eq. (31).

### C. The coherent matrix elements

As we have emphasized, our main goal in the present work is the investigation of the spin differential cross section. Although the coherent contribution is expected to be less important compared to the spin contribution especially for light nuclei, however, we find it interesting to evaluate the form factor  $F(u)$  [see Eq. (13)] for the three light nuclear isotopes  $^{19}\text{F}$ ,  $^{23}\text{Na}$ , and  $^{29}\text{Si}$ . The coherent process is described by the Fermi operator

$$\mathbf{T}^\lambda = \sqrt{4\pi} j_\lambda(qr) Y_\lambda(\hat{r}).$$

The multipole  $\lambda=0$  is the only one that contributes to  $^{19}\text{F}$  and  $^{29}\text{Si}$  and is the dominant one for  $^{23}\text{Na}$ . The matrix elements of the above operator are calculated in a similar manner to that followed for the Gamow-Teller operator (see Sec. II B), using our shell model wave functions in the  $s$ - $d$  shell. The contribution of the closed core, which in our calculation is considered to be  $^{16}\text{O}$ , will be taken from [13]. Thus the nuclear form factor  $F(u)$  entering Eq. (7) is given by

$$F(u) = \frac{Z}{A} F_Z(u) + \frac{N}{A} F_N(u), \quad (34)$$

where

$$F_Z(u) = \frac{Z^c}{Z} F_Z^c(u) + \left( 1 - \frac{Z^c}{Z} \right) F_Z^{\text{val}}(u), \quad (35)$$

$$F_N(u) = \frac{N^c}{N} F_N^c(u) + \left( 1 - \frac{N^c}{N} \right) F_N^{\text{val}}(u). \quad (36)$$

The superscripts  $c$  and  $\text{val}$  denote the contribution coming from the core and the valence particles of the  $s$ - $d$  shell, respectively. The functions  $F_{Z,N}^c$ , which describe the core contribution, are given in Ref. [13]. The quantities  $F_{Z,N}^{\text{val}}$  are the valence form factors for protons ( $Z$ ) and neutrons ( $N$ ) and they are calculated using our shell model wave functions. Their analytic expressions are found to be

$$F_Z^{\text{val}}(u) = \left[ \left( \frac{1}{15} + \Lambda_Z^{\text{val}} \right) u^2 - \frac{2}{3} u + 1 \right] e^{-u/2} \quad (37)$$

and

$$F_N^{\text{val}}(u) = \left[ \left( \frac{1}{15} + \Lambda_N^{\text{val}} \right) u^2 - \frac{2}{3} u + 1 \right] e^{-u/2}. \quad (38)$$

The coefficients  $\Lambda_a^{\text{val}}$ ,  $a=Z,N$  are calculated in a manner quite similar to the one used for the spin matrix element discussed above.

We note that the nuclear matrix element relevant for the coherent  $\chi$ -nucleus scattering is given by

$$\mathcal{M} = f_S^0 [ZF_Z(u) + NF_N(u)] + f_S^1 [ZF_Z(u) - NF_N(u)] \quad (39)$$

or

$$\mathcal{M} = A \left\{ f_S^0 + f_S^1 \frac{Z[F_Z(u) + F_N(u)] - AF_N(u)}{AF(u)} \right\} F(u). \quad (40)$$

Assuming now that  $F_Z(u) \approx F_N(u) \approx F(u)$ , as is the case for light nuclei where  $N \approx Z$ , we obtain

$$\mathcal{M} = A \left[ f_S^0 + f_S^1 \frac{2Z - A}{A} \right] F(u) \quad (41)$$

which has been used in expression (7).



Using Eqs. (34)–(38) for the contribution of the valence nucleons and the closed core contribution we find the following analytic expression for the nuclear form factor:

$$F(u)=[(\beta_{csm} + \delta)u^2 - \zeta u + 1]e^{-u/2}. \quad (42)$$

The parameter  $\zeta$  is independent of the interaction used and depends only on the bulk parameters describing the nucleus, i.e.,

$$\zeta = \frac{A^{\text{val}} + A - 4}{3A}, \quad (43)$$

where  $A^{\text{val}}$  refers to the valence nucleons of the  $s$ - $d$  shell.  $\beta_{csm}$  arises by approximating the contribution of the nucleons outside the closed shell to that of a suitable fraction  $A_j/(2j+1)$  of the  $j$ -shell contribution as given in Ref. [13], where  $A_j$  is the number of nucleons occupying the unfilled  $j$  shell.  $\delta$  is the needed correction resulting from the present exact  $s$ - $d$  shell model calculation. These parameters will be discussed in Sec. IV B.

### III. THE SHELL MODEL NUCLEAR WAVE FUNCTIONS

The evaluation of the needed matrix elements in the scattering cross section of Eq. (5) requires reliable nuclear wave functions, the construction of which is accomplished in the framework of shell model. Specifically, in our calculation we considered as model space the  $s$ - $d$  shell and utilized as effective interaction the universal  $s$ - $d$  shell interaction of Wildenthal [23] which has meticulously been developed and tested over many years. This interaction is known to accurately reproduce many nuclear observables for  $s$ - $d$  shell nuclei. The Wildenthal two-body matrix elements as well as the single particle energies are determined by least square fits to experimental data in nuclei from  $A = 17$  to  $A = 39$ .

To test the wave functions of the nuclei under consideration we compute their energy spectra and ground state magnetic moments. In Fig. 1 we present the calculated and measured [24] energy spectra for the lowest eigenstates of  $^{19}\text{F}$ ,  $^{23}\text{Na}$ , and  $^{29}\text{Si}$ . We see that in general good agreement is achieved both with experiment and previous calculations [22].

Since in our calculation we are primarily interested in the spin matrix element, it is important to compare the predicted and the measured ground state magnetic moment of the considered nuclei. The magnetic moment is defined by

$$\mu = \langle JJ | g_n^s \mathbf{S}_n + g_n^l \mathbf{L}_n + g_p^s \mathbf{S}_p + g_p^l \mathbf{L}_p | JJ \rangle \mu_N, \quad (44)$$

where the  $\mathbf{S}_i$  are the total  $z$  projection of the spin operators and  $\mathbf{L}_i$  the analogous orbital angular momentum operators. The free particle  $g$  factors are given by

$$g_n^s = -3.826, \quad g_n^l = 0.0, \quad g_p^s = 5.586, \quad g_p^l = 1.0.$$

The obtained results for the ground state magnetic moment are presented in Table III for each nucleus using the convention

$$\langle \mathbf{S} \rangle \equiv \langle J | \mathbf{S} | J \rangle = \langle JM_J = J | S_z | JM_J = J \rangle \quad (45)$$

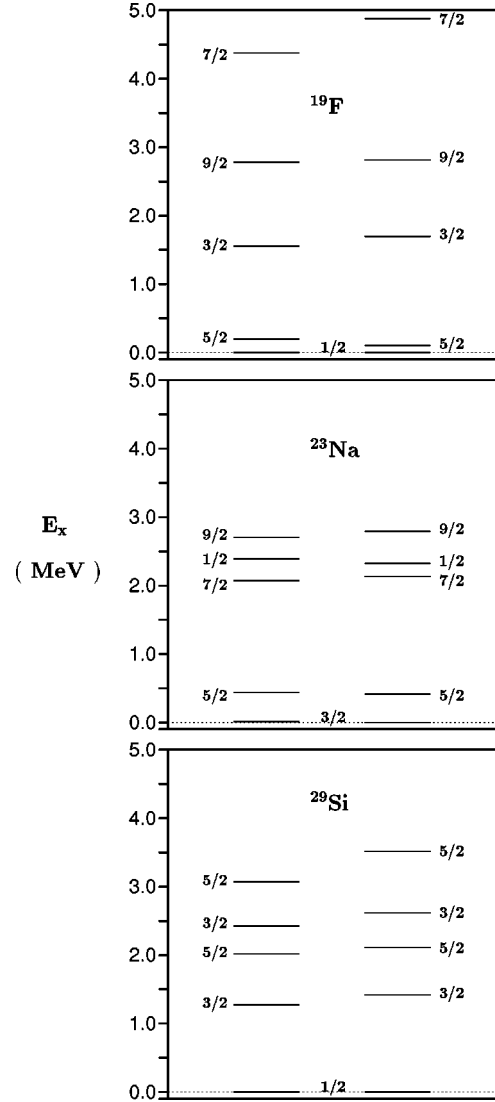


FIG. 1. The calculated (right) and measured (left) [24] energy spectra for the five lowest positive parity states of  $^{19}\text{F}$ ,  $^{23}\text{Na}$ , and  $^{29}\text{Si}$ .

and similarly for the  $\mathbf{L}$  operator. We note that neutrons contribute almost negligibly to the relevant magnetic moments of  $^{19}\text{F}$  and  $^{23}\text{Na}$ , in contrast to  $^{29}\text{Si}$  where the main contribution to the magnetic moment comes from the neutrons. In general we see that there is a very satisfactory agreement between the theoretical predictions and the experimental results.

From the definition of  $\mu$  it is apparent that we cannot make a direct comparison between the experimentally observed magnetic moment and the spin matrix element since the first involves also the orbital matrix element. For this reason, in the last column of Table III we quote the contribution of the spin component into the total value of  $\mu$ . As it can be seen, the spin component dominates in  $^{19}\text{F}$  and  $^{29}\text{Si}$  nuclei, but in the case of  $^{23}\text{Na}$  the calculated contribution of orbital angular momentum is found to be about 43% of the total value. From the above discussion we may infer that the calculated static value of the spin matrix element is reliable for the case of  $^{19}\text{F}$  and  $^{29}\text{Si}$ . Such a conclusion cannot be

TABLE III. Calculated ( $\mu$ ) and measured ( $\mu_{\text{exp}}$ ) magnetic moments. The nuclear spin and orbital angular momentum matrix elements for protons and neutrons are also presented. In the last column we quote the portion of the spin component into the total value of  $\mu$ .

Nucleus	$\langle \mathbf{S}_n \rangle$	$\langle \mathbf{S}_p \rangle$	$\langle \mathbf{L}_n \rangle$	$\langle \mathbf{L}_p \rangle$	$\mu$	$\mu_{\text{exp}}$	
$^{19}\text{F}$	-0.0087	0.4751	-0.1899	0.2235	2.91	+2.628866(8)	91%
$^{29}\text{Si}$	0.1334	-0.0019	0.3498	0.0183	-0.50	-0.55529 (3)	99%
$^{23}\text{Na}$	0.0199	0.2477	0.3207	0.9115	2.22	+2.217520(2)	57%

reached for  $^{23}\text{Na}$  due to the large contribution of the orbital angular momentum.

A further test is provided by the magnitude of the magnetic moment. If it is not quenched compared to some canonical value, e.g., the magnitude of its reduced matrix element in Weisskopf units, one can be more confident that it will be quite stable against the variation of the parameters of the nuclear model. The calculated values are 3.344 W.u for  $^{19}\text{F}$ , 1.079 W.u for  $^{23}\text{Na}$ , and 0.099 W.u for  $^{29}\text{Si}$ . From these results we see that the magnetic dipole transition is not suppressed compared to the single-particle Weisskopf value in the case of  $^{19}\text{F}$  and  $^{23}\text{Na}$ . Thus we are very confident that our wave functions for these two nuclei are quite reliable. On the other hand, in the case of  $^{29}\text{Si}$ , the suppression is quite pronounced. This gives us less confidence in the reliability of the wave function since a very small change in the ground state wave function of  $^{29}\text{Si}$  could, in principle, destroy the satisfactory agreement between theory and experiment, in spite of the fact that our results are in excellent agreement with those of the previous calculation [22], which, in our notation, are

$$[\Omega_0(0)]^2 = 0.205, \quad [\Omega_1(0)]^2 = 0.218, \quad \text{and}$$

$$\Omega_1(0)\Omega_0(0) = -0.212.$$

#### IV. RESULTS AND DISCUSSION

The presentation and analysis of our results is going to be done in two steps. First we discuss the static values entering the differential cross section, i.e., the  $q \rightarrow 0$  limit of the spin structure function (see Sec. IV A) and then we examine the behavior of both the structure function and the nuclear form factor in terms of the momentum transfer.

##### A. Static values of the cross section

For light nuclei the static value of the spin matrix element Eq. (30), obtained in the limit,  $q \rightarrow 0$  ( $u \rightarrow 0$ ), depends strongly on the nuclear structure. We exhibit these values in Table IV. In this limit the operator defined in Eq. (20) takes the simple form

$$\mathbf{O}^{(0,1)} = (f_A^0 + f_A^1 \tau_3) \boldsymbol{\sigma}. \quad (46)$$

According to Eq. (22) the reduced matrix elements of Eq. (46) for the nuclear ground state  $|g_s\rangle = |J\rangle$  are

$$\frac{\langle J || \mathbf{O}^{(0,1)} || J \rangle}{[2J+1]^{1/2}} = f_A^0 \Omega_0(0) + f_A^1 \Omega_1(0). \quad (47)$$

To compare the above definition with that of Eq. (45) we note that

$$\frac{\Omega_0(0)}{2} = (\langle JJ | \mathbf{S}_p | JJ \rangle + \langle JJ | \mathbf{S}_n | JJ \rangle) \left[ \frac{J+1}{J} \right]^{1/2} \quad (48)$$

and

$$\frac{\Omega_1(0)}{2} = (\langle JJ | \mathbf{S}_p | JJ \rangle - \langle JJ | \mathbf{S}_n | JJ \rangle) \left[ \frac{J+1}{J} \right]^{1/2}, \quad (49)$$

quantities of Table IV.

As can be seen from Table IV, both the isoscalar  $[\Omega_0(0)]^2$  and isovector  $[\Omega_1(0)]^2$  channels as well as the product  $\Omega_0(0)\Omega_1(0)$  have almost the same magnitude for each nuclear system. We also note that the static values of both channels are much quenched in the cases of  $^{29}\text{Si}$  and  $^{23}\text{Na}$  as compared to those of  $^{19}\text{F}$ . Thus the quantity  $[\Omega_1(0)]^2$  for  $^{19}\text{F}$  is a factor of about 8 and 13 greater than that of  $^{23}\text{Na}$  and  $^{29}\text{Si}$ , respectively. In Table IV we also quote the static values of two heavy nuclear systems  $^{73}\text{Ge}$  [22] and  $^{207}\text{Pb}$  [11], which are also promising cold dark matter detection targets. An overall survey of the results shows that  $^{19}\text{F}$  has the largest static value of all, while sizable quenching appears in  $^{29}\text{Si}$  and  $^{207}\text{Pb}$ . This shows that  $^{19}\text{F}$  is quite favorable LSP detection target since (i) the spin matrix element can be reliably obtained (see Sec. III) and (ii) because the static value of the spin matrix element in this case is much larger compared to those of  $^{23}\text{Na}$  and  $^{29}\text{Si}$ .

As we have already mentioned in Sec. II, the functions  $F_{\rho\rho'}(u)$  are, up to term linear in  $u$  (quadratic in the momentum transfer  $q$ ), independent of the isospin channel. We thus expect the quantity  $S(u)$  to be independent of  $u$ , i.e.,  $S(u) \approx S(0)$ . In addition, since in Eq. (13) we have factored out  $(f_A^1)^2$ , we expect  $S(0)$  to be less dependent on SUSY param-

TABLE IV. The static spin matrix elements for the light nuclei considered here. For comparison we also quote the results for the medium heavy nucleus  $^{73}\text{Ge}$  [22] and the heavy nucleus  $^{207}\text{Pb}$  [11].

	$^{19}\text{F}$	$^{29}\text{Si}$	$^{23}\text{Na}$	$^{73}\text{Ge}$	$^{207}\text{Pb}$
$[\Omega_0(0)]^2$	2.610	0.208	0.478	1.157	0.305
$[\Omega_1(0)]^2$	2.807	0.220	0.346	1.005	0.231
$\Omega_0(0)\Omega_1(0)$	2.707	-0.214	0.406	-1.078	-0.266

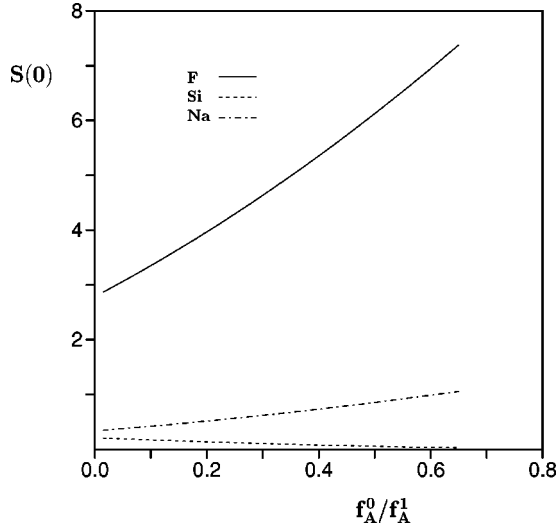


FIG. 2. The spin structure function  $S(u=0)$  versus  $f_A^0/f_A^1$  for the three isotopes  $^{19}\text{F}$ ,  $^{23}\text{Na}$ , and  $^{29}\text{Si}$ .

eters, at least as far as the dependence of the ratio  $f_A^0/f_A^1$  on the overall mass scales is concerned. In Fig. 2 we plot the quantity  $S(0)$  as a function of  $f_A^0/f_A^1$  over a range of values which we expect to be representative [10] in the SUSY allowed parameter space. In going from the quark to the nucleon level, there is some ambiguity in the case of the isoscalar matrix element (“nucleon spin crisis”). So we used two rather extreme cases in estimating the ratio  $f_A^0/f_A^1$ , i.e., the EMC (European Muon Collaboration) results and the naive quark model (NQM) [25] prediction. The isovector is renormalized in the usual way ( $g_A = 1.24$ ). Thus we find that the ratio  $f_A^0/f_A^1$  lies between the values  $(f_A^0/f_A^1)_{\min} = 0.0134$  and  $(f_A^0/f_A^1)_{\max} = 0.6685$ .

From Fig. 2 we see that  $S(0)$  is being a decreasing function of  $f_A^0/f_A^1$  for  $^{29}\text{Si}$  in contrast to the corresponding functions of  $^{19}\text{F}$  and  $^{23}\text{Na}$ . This is due to the fact that the product  $\Omega_0\Omega_1$  is negative for  $^{29}\text{Si}$  and positive for  $^{19}\text{F}$  and  $^{23}\text{Na}$ . On the other hand, the isoscalar and isovector coupling constants  $f_A^0$  and  $f_A^1$  take the same sign (positive) in all the above SUSY models. The values of  $S(0)$  lie in the regions

$$2.866 \leq S(0) \leq 7.461 \quad (^{19}\text{F}),$$

$$0.026 \leq S(0) \leq 0.204 \quad (^{29}\text{Si}),$$

$$0.347 \leq S(0) \leq 1.068 \quad (^{23}\text{Na}).$$

Particle physicists and astrophysicists tend to write the ground state spin matrix element as  $\alpha_{\rho\rho'}(J+1)J$ . There is, of course, no reason to expect this form for the spin matrix element, but one can always do this provided that the true nuclear structure effects are absorbed in the parameter  $\alpha_{\rho\rho'}$ . To satisfy this convention we give the corresponding values of  $\alpha_{\rho\rho'}$  for each isospin channel:

$$^{19}\text{F}: \quad \alpha_{11} = 3.742, \quad \alpha_{00} = 3.480, \quad \alpha_{01} = 3.609, \quad (50)$$

$$^{29}\text{Si}: \quad \alpha_{11} = 0.292, \quad \alpha_{00} = 0.276, \quad \alpha_{01} = -0.284, \quad (51)$$

$$^{23}\text{Na}: \quad \alpha_{11} = 0.092, \quad \alpha_{00} = 0.127, \quad \alpha_{01} = 0.108. \quad (52)$$

As expected, the above parameters do not show any canonical behavior. In fact they are different for the two nuclei  $^{19}\text{F}$  and  $^{29}\text{Si}$  even though they have the same spin  $J=1/2$ .

From the above discussion it is clear that, in the case of the spin dependent contribution, for small LSP mass the target  $^{19}\text{F}$  is very favored. This advantage may be lost for large LSP mass since the total cross section is proportional to the square of the reduced mass (see Ref. [12]). It is partly lost if both the isoscalar and isovector elementary couplings are equal. It is, however, completely lost if one isospin channel becomes dominant. Thus, if we consider the special case  $f_A^0=0$ , which is not unreasonable due to the suppression of the isoscalar mode coming from the EMC effect in going from the quark to the nucleon level, we find that the spin induced cross section for  $^{73}\text{Ge}$  and  $^{207}\text{Pb}$  are, respectively, four and three times larger compared to that of  $^{19}\text{F}$ .

### B. Momentum dependence of the cross section

Since the mass of the LSP is not known but it is expected to be larger than 30 GeV, the momentum transfer  $q$  becomes comparable to the inverse of the nuclear size. Therefore, finite momentum transfer must also be considered in the  $\chi$ -nucleus scattering.

The momentum dependence of the differential cross section in the present work is realized in two steps. At first step we examine the momentum dependence of each multipole  $\lambda$  by considering the ratio  $R^{(\lambda,k)}(u) \equiv \Omega_1^{(\lambda,k)}(u)/\Omega_1(0)$ . In the second step we investigate the behavior of the structure functions  $F_{\rho\rho'}(u)$  with  $\rho, \rho' = 0, 1$  as well as the square of the nuclear form factor  $|F(u)|^2$ .

Before discussing the results let us first find the upper limit of the momentum transfer corresponding to the nuclei we examine in the present paper. There are two restrictions for the maximum allowed momentum transfer. The first one is the mass of LSP,  $m_\chi$ , and the second is its velocity  $v$ . As  $m_\chi$  becomes much greater than the nuclear mass  $Am_N$ , the reduced mass  $\mu_r$  asymptotes to  $\mu_r \rightarrow Am_N$ . As we have said, it is expected that the LSP will obey Maxwell-Boltzmann distribution. Since, however, the LSP is trapped in the gravitational field of the galaxy, we have velocities less than the velocity  $v_{esc} = 625$  km/s which is almost  $2\sqrt{\langle v \rangle^2}$ , where  $\sqrt{\langle v \rangle^2} = 10^{-3}c$ . Therefore, the maximum value of  $u$  is  $u_{\max} = 2(v_{esc}\mu_r b)^2$ . For the nuclei considered here the maximum values of  $u$  for  $m_\chi \gg Am_N$  are correspondingly

$$u_{\max}(^{19}\text{F}) \sim 0.17, \quad u_{\max}(^{23}\text{Na}) \sim 0.30, \quad u_{\max}(^{29}\text{Si}) \sim 0.50,$$

where the oscillator parameter  $b$  is determined from the phenomenological equation  $b = 1.00A^{1/6}$ , which yields

$$b(^{19}\text{F}) = 1.63 \text{ fm}, \quad b(^{23}\text{Na}) = 1.69 \text{ fm}, \text{ and}$$

$$b(^{29}\text{Si}) = 1.75 \text{ fm}. \quad (53)$$

Another more sophisticated formula [27] commonly used yields



$$b(^{19}\text{F})=1.71 \text{ fm}, \quad b(^{23}\text{Na})=1.16 \text{ fm}, \text{ and}$$

$$b(^{29}\text{Si})=1.85 \text{ fm} \quad (54)$$

(for other formulas see Lalazisis and Panos [28]). We should also mention that there is a minimum value of  $u$  which comes from the detector energy cutoff  $Q_{\min}$  [see Eqs. (12)]. In the present work we will consider  $Q_{\min}=10$  keV. Then

$$u_{\min}(^{19}\text{F})\sim 0.011, \quad u_{\min}(^{23}\text{Na})\sim 0.015,$$

$$u_{\min}(^{29}\text{Si})\sim 0.021.$$

It is thus clear that, for light systems, the detection rate is greatly suppressed in the presence of cutoff. For the  $u$  dependence of the differential rate we note that the  $\lambda=0$  multipole in  $F_{11}(u)$ , falls as  $u$  increases. Can this be partly counteracted by the multipoles with  $\lambda \neq 0$  which initially increase as functions of  $u$ ?

Let us begin our discussion in the limit of infinite pion mass (usual axial current). In Fig. 3 we present the functions  $R^{(\lambda,k)}(u)$  versus  $u$ . We mention that the ground state of  $^{19}\text{F}$  and  $^{29}\text{Si}$  is the  $1/2^+$  and in  $^{23}\text{Na}$  the  $3/2^+$ . Therefore, in the case of  $^{19}\text{F}$  and  $^{29}\text{Si}$  only two multipoles,  $\lambda=0$  and  $\lambda=2$  with  $k=1$ , contribute, while in  $^{23}\text{Na}$  we have additional contributions from the multipoles  $\lambda=2,4$  with  $k=3$ .

As can be seen from Fig. 3,  $R^{(2,1)}(u)$  is negligible for  $^{19}\text{F}$ . Therefore, it cannot affect the momentum dependence of the spin response function. We note, however, that this function decreases very little taking the value  $0.82 \times 0.82 = 0.67$  for the highest  $u$  (see Fig. 3). The same is true for  $^{23}\text{Na}$  as far as the  $R^{(2,1)}(u)$  is concerned, but in this case one has a sizable positive contribution due to the  $R^{(2,3)}(u)$ . This will tend to somewhat counteract the decrease of the usual,  $\lambda=0$ , spin contribution as  $u$  increases. The net effect, however, is not significant since the various multipoles do not interfere (their squares add). Therefore, near the end point the cross section drops significantly.

In the case of  $^{29}\text{Si}$ ,  $R^{(2,1)}(u)$  increases a bit faster than in the previous two nuclei but we see that again this is not enough to offset the reduction of the leading usual spin contribution at the highest possible  $u=0.5$ . The above effects explain the behavior of the structure function  $F_{11}(u)$  as a function of  $u$ ; see Fig. 4 for the three nuclei considered in this work (the  $u$  dependence of the other isospin structure functions  $F_{\rho\rho'}$  is similar). One can see that, for LSP heavier than the nuclei considered, near the end point the suppression of the differential rate arising from the energy transfer dependence of spin contribution is not negligible. In other words, in the limit of infinite pion mass, the differential rate can be decreased up to about 33% at  $u=0.17$  for  $^{19}\text{F}$ , 48% at  $u=0.30$  for  $^{23}\text{Na}$  and 64% at  $u=0.5$  for  $^{29}\text{Si}$ .

Following Ref. [22] we could, of course, have also attempted a parametrization of the spin form factors  $F_{\rho\rho'}$  using only exponentials  $e^{-\lambda_{\rho\rho'}u}$  in a given range of  $u$ . We did not do this for two reasons: (i) As the authors of Ref. [22] warn, the fit would be valid only in that interval of  $u$ . For this reason a comparison of the momentum dependence of our results with previous ones will not be attempted. (ii) In ob-

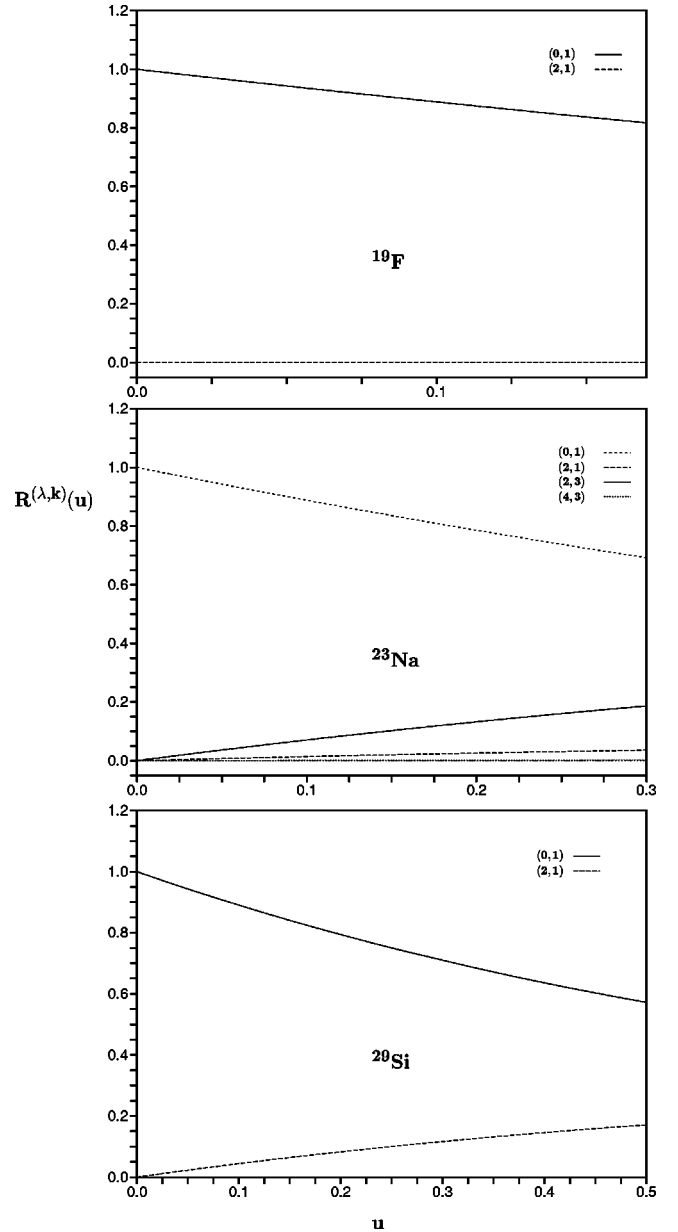


FIG. 3. Behavior of the ratio  $R^{(\lambda,k)}(u) \equiv \Omega_1^{(\lambda,k)}(u)/\Omega_1(0)$  as a function of  $u$ : (i)  $^{19}\text{F}$  contributions for  $\lambda=0,2$  and  $k=1$ , (ii)  $^{23}\text{Na}$  contributions for  $\lambda=0,2$ , with  $k=1$  and for  $\lambda=2,4$  with  $k=3$ , and (iii)  $^{29}\text{Si}$  contributions  $\lambda=0,2$  and  $k=1$ . These are the only possible multipoles contributing for each isotope.

taining the total from the differential rate, one must combine the spin form factors with functions like those of Eqs. (39)–(41) of Ref. [12]. Thus, handling exponentials is not substantially simpler, especially for numerical purposes.

Let us now briefly discuss the effect of the finite pion mass (PCAC effect). From our discussion in Sec. II B it is clear that the spin response function will drop a bit faster as a function of  $u$ . In general, one can have interference of the different  $\lambda$ -multipoles associated with the same  $k$ . In the examples considered here, we find that the interference between the  $\lambda=0$  and  $\lambda=2$  multipoles is negligible. The drop observed in the spin cross section is mainly due to the reduc-

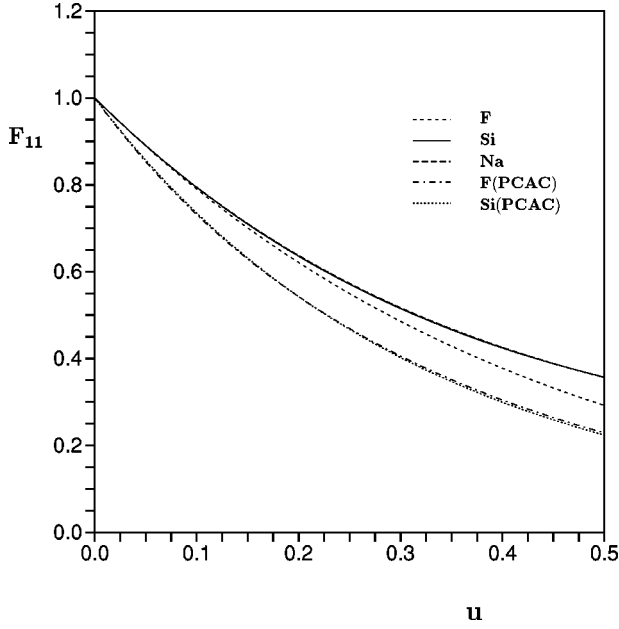


FIG. 4. Isovector nuclear spin form factor  $F_{11}(u)$  versus  $u$ , for the isotopes,  $^{19}\text{F}$  ( $0.011 \leq u \leq 0.17$ ),  $^{23}\text{Na}$  ( $0.015 \leq u \leq 0.30$ ), and  $^{29}\text{Si}$  ( $0.021 \leq u \leq 0.50$ ). The behavior of the other isospin structure functions  $F_{\rho\rho'}$  with  $\rho, \rho' = 0, 1$  is similar. In this figure we also plot the function  $F_{11}(u)$  for  $^{19}\text{F}$  and  $^{29}\text{Si}$  when PCAC effect is considered.  $u$  is related to the energy transfer  $Q$  via Eq. (12).

tion of the dominant  $\lambda=0$  multipole. For comparison this modified momentum dependence of the isovector channel is also given in Fig. 4 for the isotopes  $^{19}\text{F}$  and  $^{29}\text{Si}$ . The effect of PCAC is to further reduce the rate near the end point by 13% for  $^{19}\text{F}$  and by 40% for  $^{29}\text{Si}$ .

Finally, as we have mentioned in Sec. II C, the coherent contribution is described in terms of the nuclear form factor  $F(u)$ . This is described in terms of the gross properties (the mass number  $A$  and the number of valence nucleons  $A^{\text{val}}$  in the  $s$ - $d$  shell) and the parameters  $\beta_{csm}$  and  $\delta$ . For the nuclei considered in this work the latter two parameters are given in Table II. From this table we see that  $\delta$  is quite small, which means that the approximation of Ref. [13], which puts the nucleons of the three isotopes  $^{19}\text{F}$ ,  $^{23}\text{Na}$ , and  $^{29}\text{Si}$  in the lowest orbits allowed by the Pauli principle, is quite adequate.

As a test of the reliability of the above form factor, Eq. (42), one can calculate the experimentally measured mean square radius [29]  $\langle r^2 \rangle = -6dF/dq^2$  evaluated at  $q=0$ . One finds that within the  $1s$ - $0d$  model space this quantity is independent of the interaction employed. In fact it is easy to show, using Eqs. (11) and (42), that

$$\langle r^2 \rangle = (3\zeta + 1.5)b^2. \quad (55)$$

Thus Eq. (54) and the values of  $\zeta$  from Table II yield (in fm's)

$$\langle r^2 \rangle^{1/2} = 2.55, 2.74, 2.93 \text{ for } ^{19}\text{F}, ^{23}\text{Na}, ^{29}\text{Si}, \quad (56)$$

respectively, which compares well with the experimentally determined values [29] (in fm's)

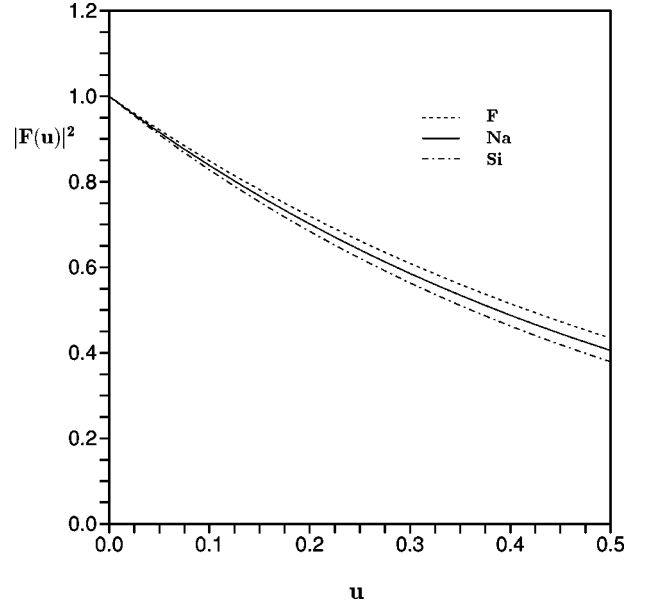


FIG. 5. The square of the nuclear form factor  $|F(u)|^2$  versus  $u$ , for the isotopes  $^{19}\text{F}$ ,  $^{23}\text{Na}$ , and  $^{29}\text{Si}$ .

$$\langle r^2 \rangle^{1/2} = 2.90, 2.94, 3.09 \text{ for } ^{19}\text{F}, ^{23}\text{Na}, ^{29}\text{Si}, \quad (57)$$

respectively. The small discrepancy is not troublesome since the differential event rate is less sensitive to such parameters.

Using the results of our calculation, in Fig. 5 we plot the square of the nuclear form factor,  $|F(u)|^2$ , as a function of  $u$  for the above three isotopes. As can be seen, the dependence of  $|F(u)|^2$  on  $u$  is less dramatic compared to that of the spin structure function (Fig. 4). This is attributed to the fact that  $\zeta$  of Eq. (42) is approximately a factor of two smaller than the corresponding term of the spin function.

## V. SUMMARY AND CONCLUSIONS

In the present paper our main effort has focused on the calculation of the spin contribution to the differential cross section for supersymmetric dark matter detection in the case of three light experimentally interesting targets  $^{19}\text{F}$ ,  $^{23}\text{Na}$ , and  $^{29}\text{Si}$ .

Our nuclear wave functions were obtained by shell model calculations in the  $s$ - $d$  shell using the Wildenthal interaction. These wave functions accurately describe the relevant experimental data (low energy spectra and ground state magnetic moments). So, we view the obtained spin matrix elements as sufficiently accurate.

The nuclear structure dependence of the differential cross section is adequately described by a function  $S(u)$ ,  $u$  being proportional to the energy transfer. This quantity,  $S(u)$ , was judiciously defined so that it is essentially static and depends mildly on the parameters of supersymmetry. From this point of view we find that the most favorable target is  $^{19}\text{F}$  which is due to the fact that its spin matrix element is not quenched. Furthermore, the various isospin channels add coherently. For the other two nuclei,  $^{23}\text{Na}$  and  $^{29}\text{Si}$ , the spin matrix element is suppressed but not unusually small.

We discussed in addition the dependence of the cross

section on the energy transfer to the nucleus [defined by Eq. (12)]. We found that, if the three isospin structure functions  $F_{\rho\rho'}$  associated with the spin, are suitably normalized, so that their value at zero energy transfer ( $u=0$ ) is one, they show very similar dependence on the energy transfer. So we focused our attention on the isovector form factor  $S_{11}(u)$ . We found that its sensitivity to the energy transfer to the nucleus is milder than in the case of heavier nuclei. Near the end point, however, it can be decreased by about 50%, which becomes about 60%, when PCAC effect is taken into account. We made no attempt to study the third ingredient of the spin contribution, namely the factor  $f_A^1$ , which of course carries the bulk of the dependence on the parameters of supersymmetry and is very sensitive to them.

Finally we studied the dependence of the coherent scattering cross section on the nuclear structure, i.e., the nuclear form factor. This scales with  $A$  and, as a result, the coherent process is going to be more important for heavy nuclei, especially if the dark matter particles are light so that the effects of the form factor are rather mild. The drop of the square of the form factor as a function of  $u$  is less dramatic compared to that of the spin structure function. This also tends to favor the coherent mode for higher  $u$ .

The detection rate for the coherent process depends critically on the parameter  $f_S^0$ , which is also sensitive to the not so well known input parameters of supersymmetry. We did not address such issues in this work. Thus, we cannot say whether this process is detectable or even how the coherent contribution compares with the spin contribution.

In conclusion, we have demonstrated that the dependence on the nuclear structure of the LSP-nucleus elastic scattering cross section can be reliably calculated, both for the coherent as well as the spin mode, especially for light nuclei. Using realistic shell model wave functions one can obtain both the static values as well as the energy transfer dependence. To obtain the event rates one must combine our results with realistic calculations in the allowed supersymmetric parameter space. The latter will be considered elsewhere.

## ACKNOWLEDGMENTS

Partial support by the Greek State Scholarships Foundation for one of the authors (P.C.D) and PENEΔ 95 (for J.D.V. and P.C.D.) is gratefully acknowledged. P.C.D. would also like to thank the University of Ioannina and NCSR Demokritos for hospitality.

## APPENDIX

The reduced matrix elements  $\langle j_2 || T^{(l,S)J} || j_1 \rangle$  both for the coherent  $S=0$  and spin  $S=1$  operators in the harmonic oscillator basis can be written as

$$\langle j_2 || \hat{T}^{(l,S)J} || j_1 \rangle = e^{-\chi} \sum_{\kappa=0}^{\kappa_{\max}} \theta_{\kappa}^S \chi^{\kappa+1/2}, \quad \chi = (qb)^2/4, \quad (\text{A1})$$

with

$$\theta_{\kappa}^S(j_1 j_2; J) = \hat{j}_1 \hat{j}_2 \hat{J} (S+1)^{1/2} (S+2)^{1/2} \left\{ \begin{array}{ccc} l_2 & \frac{1}{2} & j_2 \\ l_1 & \frac{1}{2} & j_1 \\ l & S & J \end{array} \right\} \times \langle l_2 || \sqrt{4\pi} Y^l || l_1 \rangle \varepsilon_{\kappa} \quad (\text{A2})$$

and

$$\kappa_{\max} = n_1 + n_2 + m, \quad m = (l_1 + l_2 - l)/2. \quad (\text{A3})$$

The coefficients  $\varepsilon_{\kappa}(n_1 l_1, n_2 l_2, l)$  are simple numbers [11]. This compact formula provides the advantage of computing  $\theta_{\kappa}^S$ , which are independent of the momentum  $q$ , once for our model space. Then the necessary matrix elements  $\langle j_2 || \hat{T}^J || j_1 \rangle$  are easily evaluated for every value of the momentum transfer  $q$  or equivalently the variable  $u$ .

- 
- [1] E.W. Kolb and M.S. Turner, *The Early Universe* (Addison-Wesley, Redwood City, CA, 1990); P.J.E. Peebles, *Principles of Physical Cosmology*, (Princeton University Press, Princeton, NJ, 1993).
- [2] For a recent review see, e.g., G. Jungman, M. Kamionkowski, and K. Griest, Phys. Rep. **267**, 195 (1996).
- [3] COBE data, G.F. Smoot *et al.*, Astrophys. J. Lett. **396**, L1 (1992).
- [4] E. Gawser and J. Silk, Science **280**, 1405 (1988); M.A.K. Gross, R.S. Somerville, J.R. Primack, J. Holtzman, and A.A. Klypin, Mon. Not. R. Astron. Soc. **301**, 81 (1998).
- [5] R.S. Somerville, J.R. Primack, and S.M. Faber, astro-ph/9806228.
- [6] L. M. Krauss, in *The New Cosmology and Dark Matter*, Proceedings of the 2nd International Workshop on the Identification of Dark Matter, Buxton, UK, 1998, edited by N.J.C. Spooner and V. Kudryavtsev (World Scientific, Singapore, 1999), p. 1.
- [7] D.P. Bennett *et al.*, MACHO Collaboration, in *Dark Matter*, Proceedings of the 5th Annual Maryland Conference, College Park, MD, 1994, edited by S. S. Holt and C. L. Bennett, AIP Conf. Proc. No. 336 (AIP, New York, 1995), p. 336; C. Alcock *et al.*, MACHO Collaboration, Phys. Rev. Lett. **74**, 2867 (1995).
- [8] R. Bernabei *et al.*, Phys. Lett. B **389**, 757 (1996).
- [9] R. Bernabei *et al.*, Phys. Lett. B **424**, 195 (1998).
- [10] J.D. Vergados, J. Phys. G **22**, 253 (1996); J.D. Vergados and T.S. Kosmas, Yad. Fiz. **61**, 1166 (1988) [Phys. At. Nucl. **61**, 1066 (1998)].
- [11] T.S. Kosmas and J.D. Vergados, Phys. Rev. D **55**, 1752 (1997).
- [12] J.D. Vergados, Phys. Rev. D **58**, 103001 (1998).
- [13] T.S. Kosmas and J.D. Vergados, Nucl. Phys. **A536**, 72 (1992).
- [14] K. Griest, Phys. Rev. Lett. **61**, 666 (1988); Phys. Rev. D **38**, 2357 (1988); **39**, 3802 (1989).

- [15] A.K. Drukier, K. Freese, and D.N. Spergel, *Phys. Rev. D* **33**, 3495 (1986).
- [16] K. Freese, J. Frieman, and A. Gould, *Phys. Rev. D* **37**, 3388 (1988).
- [17] J. Ellis and R.A. Flores, *Phys. Lett. B* **263**, 259 (1991).
- [18] J. Engel and P. Vogel, *Phys. Rev. D* **40**, 3132 (1989).
- [19] J. Ellis and R.A. Flores, *Nucl. Phys.* **B307**, 883 (1988).
- [20] A.F. Pacheco and D. Strottman, *Phys. Rev. D* **40**, 2131 (1989).
- [21] F. Iachello, L.M. Krauss, and G. Maino, *Phys. Lett. B* **254**, 220 (1991).
- [22] M.T. Ressell, M.B. Aufderheide, S.D. Bloom, K. Griest, G.J. Mathews, and D.A. Resler, *Phys. Rev. D* **48**, 5519 (1993).
- [23] B.H. Wildenthal, *Prog. Part. Nucl. Phys.* **11**, 5 (1984).
- [24] R. Firestone, V.S. Shirley, and F. Chu, *Table of Isotopes* (Wiley, New York, 1996).
- [25] J. Ashman *et al.*, EMC Collaboration, *Nucl. Phys.* **B328**, 1 (1989).
- [26] B.A. Brown, B.H. Wildenthal, C.F. Williamson, F.N. Rad, and S. Kowalski, *Phys. Rev. C* **32**, 1127 (1985).
- [27] W.H. Hornyak, *Nuclear Structure* (Academic, New York, 1975).
- [28] G.A. Lalazisis and C.P. Panos, *Phys. Rev. C* **51**, 1247 (1995).
- [29] H. de Vries, C.W. de Jager, and C. de Vries, *At. Data Nucl. Data Tables* **36**, 495 (1987).